



OPEN

SUBJECT AREAS:

LASERS, LEDS AND LIGHT
SOURCES

NANOWIRES

Received
14 October 2014Accepted
5 January 2015Published
16 February 2015Correspondence and
requests for materials
should be addressed to
Z.M. (zetian.mi@
mcgill.ca)

Aluminum nitride nanowire light emitting diodes: Breaking the fundamental bottleneck of deep ultraviolet light sources

S. Zhao¹, A. T. Connie¹, M. H. T. Dastjerdi¹, X. H. Kong², Q. Wang¹, M. Djavid¹, S. Sadaf¹, X. D. Liu³, I. Shih¹, H. Guo² & Z. Mi¹¹Department of Electrical and Computer Engineering, McGill University, 3480 University Street, Montreal, Quebec, Canada H3A 0E9,²Department of Physics, McGill University, 3600 University Street, Montreal, Quebec, Canada H3A 2T8, ³Facility for Electron Microscopy Research, McGill University, 3640 University Street, Montreal, Quebec H3A 0C7.

Despite broad interest in aluminum gallium nitride (AlGa_N) optoelectronic devices for deep ultraviolet (DUV) applications, the performance of conventional Al(Ga)_N planar devices drastically decays when approaching the AlN end, including low internal quantum efficiencies (IQEs) and high device operation voltages. Here we show that these challenges can be addressed by utilizing nitrogen (N) polar Al(Ga)_N nanowires grown directly on Si substrate. By carefully tuning the synthesis conditions, a record IQE of 80% can be realized with N-polar AlN nanowires, which is nearly ten times higher compared to high quality planar AlN. The first 210 nm emitting AlN nanowire light emitting diodes (LEDs) were achieved, with a turn on voltage of about 6 V, which is significantly lower than the commonly observed 20–40 V. This can be ascribed to both efficient Mg doping by controlling the nanowire growth rate and N-polarity induced internal electrical field that favors hole injection. In the end, high performance N-polar AlGa_N nanowire LEDs with emission wavelengths covering the UV-B/C bands were also demonstrated.

Aluminum gallium nitride (AlGa_N) has attracted significant attention for deep ultraviolet (DUV) light emitting diodes (LEDs) and laser diodes (LDs)^{1–26}, and is positioned to replace conventional mercury-based light sources for water purification, sterilization, and bio-chemical detection. To date, however, the performance of planar AlGa_N DUV devices has been fundamentally limited by the prohibitively large dislocation density and the extremely inefficient p-type doping, due to the structural and electrical properties of the end compound – AlN. As an example, compared to the relatively mature Ga_N-based blue LEDs, Al-rich AlGa_N LEDs generally exhibit very high turn on voltage. This is largely due to the large magnesium (Mg) activation energy (~0.5 eV) and extremely low Mg doping efficiency at room temperature in the end compound – AlN^{2,27}. The first demonstrated thin film AlN LEDs have a turn on voltage of more than 20 V², significantly larger than the band gap of AlN (~6 eV). Moreover, the lattice mismatch between AlN and various available substrates (e.g., sapphire, SiC) induces extremely high threading dislocation densities (TDDs) in either AlN or Al-rich AlGa_N epilayers^{6,11,28,29}, leading to poor material quality, and thus a low material internal quantum efficiency (IQE). For wavelengths in the range of 250–300 nm, the IQE can reach above 50%^{6,8,13}. However, the IQE drops very fast to less than 10% when approaching to 210 nm⁸. This eventually becomes the inherent limitation to further improve the LED performance³⁰, and to realize electrically injected lasers operating in the UV-B/C bands^{11,12}. Besides these challenges related to the properties of AlN, conventional AlGa_N DUV planar devices are Al/Ga-polar, wherein the polarization induced internal electric field is against hole injection, thus severely limiting the efficiency of hole transport.

In this letter, we demonstrate that these critical challenges can be fundamentally addressed by employing nitrogen (N) polar Al(Ga)_N nanowires spontaneously formed on large-area and low-cost Si substrate. In the N-polar configuration, the polarization induced internal electrical field is anti-parallel to the built-in electrical field of the p-top device, and can significantly enhance charge carrier transport under relatively low operation voltage. Experimentally, however, realizing such nanowire devices has remained elusive³¹. Here, we show that with an improved catalyst-free molecular beam epitaxy (MBE) process, the IQE of N-polar AlN nanowires can reach 80%



at room temperature, nearly an order of magnitude higher compared to conventional planar AlN³¹. We have further demonstrated, for the first time, AlN nanowire LEDs operating at 210 nm, the shortest wavelength ever reported for any nanostructured devices. The devices exhibit a turn on voltage of 6 V, which is only limited by the band gap of AlN. These results indicate the great potential of N-polar Al(Ga)N nanowires in future DUV optoelectronic devices.

Results

Structural characterization. Catalyst-free AlN nanowires were grown on Si substrates by radio-frequency plasma-assisted MBE under nitrogen-rich conditions. Before the growth of AlN nanowires, GaN nanowire template was first grown to promote the formation of AlN nanowires. Such a schematic is shown in Fig. 1a. Figure 1b shows the scanning electron microscope (SEM) image of AlN nanowires on GaN nanowire template. The lateral dimensions of the nanowires are about 50–60 nm. It is seen that the nanowires are highly uniform and vertically aligned, which are well suited for the fabrication of large area LED devices. Previous studies have confirmed that the majority of GaN-based nanowires grown on Si substrate by MBE under nitrogen-rich conditions have a N-polarity^{14,32–34}. Figure 1c shows the high-resolution transmission electron microscopy (TEM) image of the AlN section (10 nm above the GaN nanowire template). The crystalline planes of AlN can be clearly observed, and detailed examination further indicates the absence of stacking faults and misfit dislocations. The interplanar spacing was found to be 0.250 nm, suggesting the growth direction is along the *c*-axis^{35,36}, which is marked by the arrow.

Estimating IQE by photoluminescence experiments. Photoluminescence (PL) studies were subsequently performed on such as grown AlN nanowires. Figure 2a shows the PL spectra of AlN nanowires taken at room temperature and low temperature (20 K). Free exciton emission at 6.034 eV was observed at room temperature, which is nearly identical to that of AlN bulk crystal, suggesting AlN nanowires grown on Si substrate is strain-free³¹. By the ratio $I_{PL}(300\text{ K})/I_{PL}(20\text{ K})$, where I_{PL} is the integrated PL intensity, the room-temperature IQE is estimated to be 80%, assuming a near-unity IQE at 20 K. Figure 2b shows the IQE measured under different excitation powers. It is seen that the IQE

values remain nearly constant over a broad power range, further confirming the superior quality of the presented AlN nanowires. This measured IQE is nearly ten times higher compared to the previously reported high quality planar AlN³¹ and is also comparable to that of the state-of-the-art GaN-based blue quantum well LEDs.

p-Type doping. Another critical challenge for practical device applications is p-type doping. In this regard, the Mg dopant incorporation mechanism into AlN nanowires was first studied (see Supplementary Information for the first-principle calculation using the Vienna Ab-initio Simulation Package, VASP), and the dopant surface segregation effect^{37–40} that could enhance Mg dopant incorporation in AlN nanowires was identified. In practice, however, the Mg dopant incorporation is still difficult due to the much enhanced Mg dopant surface desorption at the elevated growth temperature⁴⁰, limiting the achievement of p-type AlN nanowires. Here we show that such a critical challenge can be overcome by carefully controlling the growth rate of AlN nanowires. The optical and electrical characteristics of three representative AlN:Mg nanowire samples are described, including samples A (growth rate 3.5 nm/min, $T_{Mg} = 280^\circ\text{C}$), B (growth rate 1.5 nm/min, $T_{Mg} = 280^\circ\text{C}$), and C (growth rate 1.5 nm/min, $T_{Mg} = 340^\circ\text{C}$) (see Methods). Shown in Fig. 2c are the Mg 1s satellite peaks taken from AlN:Mg nanowire sidewalls using angle-resolved X-ray photoelectron spectroscopy (ARXPS). It is seen that the Mg 1s peak intensity increases significantly by reducing the growth rate from 3.5 (sample A) to 1.5 nm/min (sample B), indicating an enhanced Mg surface incorporation. With further increasing Mg doping concentration (Sample C, T_{Mg} of 340°C), the Mg 1s peak intensity increases drastically. It is thus seen that by optimizing the growth conditions in particular the growth rate, the Mg surface incorporation can overcome surface desorption during the nanowire growth process, rendering high Mg concentration in AlN nanowires.

Detailed PL studies further provide unambiguous evidence for the presence of Mg acceptors in AlN nanowires. The room temperature PL spectrum of sample C is shown in Fig. 2d (solid curve). It is seen that besides the band edge PL emission peak, another low energy peak, with comparable peak intensity to the band edge PL emission peak, appears. The energy separation is about 0.5 eV, which is consistent with Mg ionization energy in AlN, i.e., the energy difference between Mg acceptor energy level and valence band maximum (VBM)^{2,27}. The Mg-acceptor related transition of Sample C (growth rate 1.5 nm/min, $T_{Mg} = 340^\circ\text{C}$) is significantly stronger than that of sample D (growth rate 3.5 nm/min, $T_{Mg} = 340^\circ\text{C}$, shown by the dashed curve), confirming that the growth rate has a dramatic influence on the Mg incorporation. It is worth noting that this is the first time that such a Mg acceptor energy level related PL emission can be clearly observed at room temperature in any AlN structures, suggesting the presence of a high Mg concentration. In addition, it is noted that nitrogen vacancies related DUV PL bands with peak wavelengths around 260–280 nm^{27,41} were not observed, further indicating a much reduced or a negligible level of nitrogen vacancies in the presented AlN:Mg nanowires. Considering the compensation effect of nitrogen vacancies^{27,41} to Mg acceptors, such a reduced or negligible level of nitrogen vacancies can naturally lead to more efficient p-type doping. The electrical measurements further show that the free hole concentration in AlN:Mg nanowires is 10^{16} cm^{-3} , or higher at room temperature (see Supplementary Information), which is orders of magnitude higher than the previous report².

Fabrication and characterization of Al(Ga)N LEDs. AlN nanowire LEDs were subsequently grown and fabricated. The device structure is schematically shown in Fig. 3a, which consists of 80 nm heavily Si-doped GaN contact layer, 90 nm Si-doped AlN, 60 nm non-doped AlN, 15 nm Mg-doped AlN, and 10 nm Mg-doped AlGaIn contact layer. For the p-AlGaIn contact layer, the Al nominal concentration

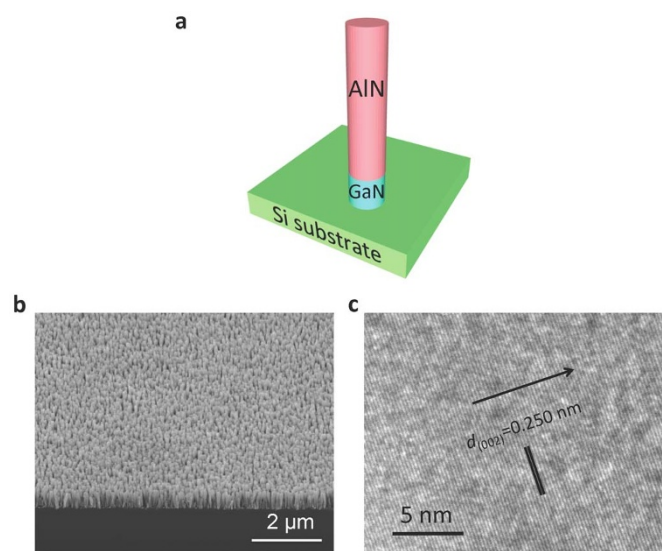


Figure 1 | Structural characterization of dislocation-free AlN nanowires. (a) The schematic of the AlN nanowire grown on GaN nanowire template on Si substrate. (b) An SEM image of such AlN/GaN nanowires grown on Si. (c) A high resolution TEM image of AlN nanowires. The arrow indicates the growth direction.

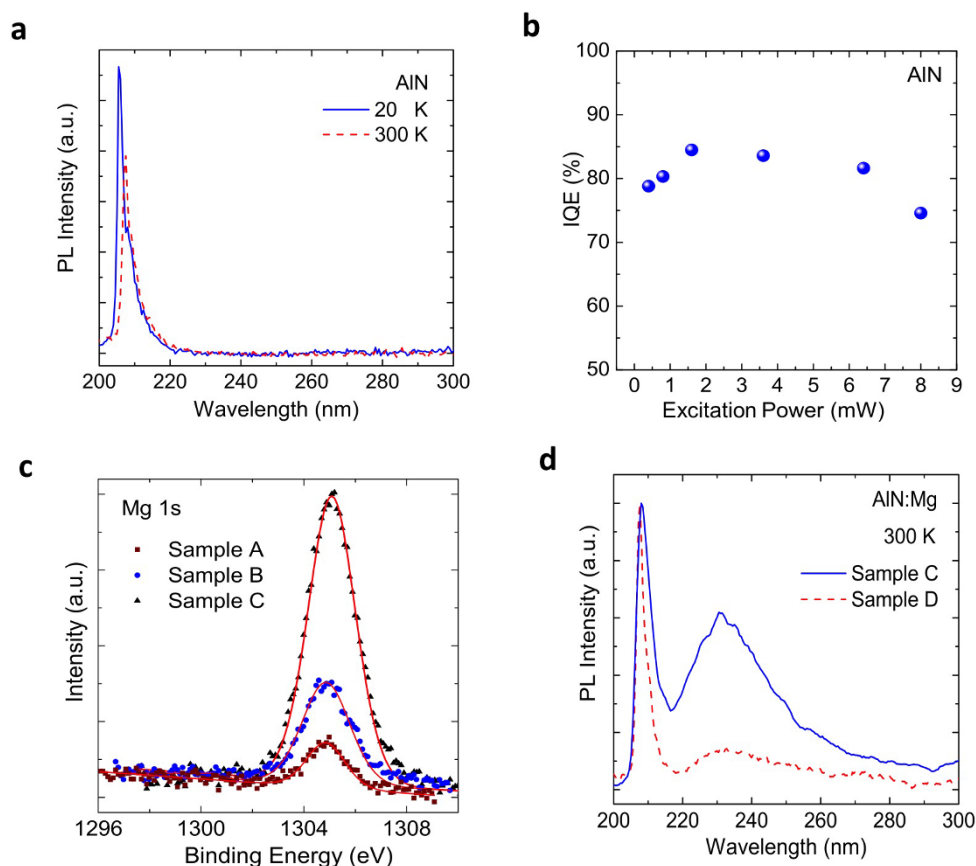


Figure 2 | Optical properties of superior quality AlN nanowires. (a) Photoluminescence (PL) spectra of AlN nanowires measured under an excitation power of 1 mW at 20 K and 300 K. (b) The derived IQE of AlN nanowires under different excitation powers. (c) Mg 1s satellite peaks in AlN:Mg nanowires. Sample A: growth rate 3.5 nm/min, $T_{\text{Mg}} = 280^\circ\text{C}$. Sample B: growth rate 1.5 nm/min, $T_{\text{Mg}} = 280^\circ\text{C}$. Sample C: growth rate 1.5 nm/min, $T_{\text{Mg}} = 340^\circ\text{C}$. (d) PL spectra taken from AlN:Mg nanowires at room temperature with an excitation of 5 mW. The PL spectra were normalized by the main PL peak of each sample. Sample C: growth rate 1.5 nm/min, $T_{\text{Mg}} = 340^\circ\text{C}$. Sample D: growth rate 3.5 nm/min, $T_{\text{Mg}} = 340^\circ\text{C}$.

by Al/(Ga+Al) flux ratio is about 20%. The corresponding SEM image and the PL spectrum of the AlN LED structure are shown in the Supplementary Information (Figs. S4 and S5). The *I*-*V* characteristics of AlN LEDs are shown in Fig. 3b, with the optical image of the probed device (size of 0.3 mm by 0.3 mm) shown in the Supplementary Information (Fig. S6). From the *I*-*V* characteristics it is seen that the turn on voltage is about 6 V, and at a forward current of 20 mA the forward voltage is only 8 V. This is in contrast to conventional planar Al-polar AlN or Al-rich AlGaIn LEDs where a turn on voltage of 20–40 V is commonly measured (e.g., Ref. 2). In addition, the reverse bias leakage current is small; a rectification ratio of nearly 10^4 was measured at ± 7 V.

The significantly improved electrical performance can be partly ascribed to the drastically enhanced Mg doping by controlling the AlN nanowire growth rate. In the path of achieving low resistance AlN LEDs, we had performed extensive studies and investigated many AlN LED structures with different growth conditions while keeping the same p-contact layer. It was found that only the devices with a relatively low growth rate for AlN layers can have low resistance. In addition, the polarization-induced field in the N-polar AlN LEDs is anti-parallel to the built-in electric field of the p-n junction, which contributes to a lower forward voltage. Detailed simulation indicates that the forward voltage at 20 mA of N-polar AlN nanowire LEDs is indeed lower than that of metal-polar AlN nanowire LEDs. Similar effects have also been observed in InGaIn/GaN quantum well LEDs^{42,43}.

Shown in Fig. 3c, strong band-edge electroluminescence (EL) emission (210 nm) was measured at room temperature under different

injection levels. The output power increases nearly linearly with increasing the injection current, illustrated in the inset of Fig. 3c. In addition, we did not measure any other emission peaks in the wavelength range from 210 nm to 260 nm. This is the first demonstration of AlN LEDs with the use of nanostructures. Such dislocation-free nanowire structures also make it possible to realize Al-rich AlGaIn emitters in the DUV spectral range with excellent electrical performance.

In this regard, we have further developed Al-rich AlGaIn nanowire LEDs with tunable emission wavelengths. The wavelength tunability can be readily realized by varying the Al compositions (see Fig. S7 in the Supplementary Information). Such AlGaIn LEDs consist of p- and n-GaN contact layers, n- and p-AlGaIn cladding layers, and i-AlGaIn active region. The typical device structure, corresponding SEM image, and room-temperature PL spectrum are shown in the Supplementary Information (Figs. S8, S9, and S10). The *I*-*V* characteristics of AlGaIn LEDs are shown in Fig. 3d. It is seen that the turn on voltage is about 5 V, and at a forward current of 20 mA the forward bias is about 6 V. The inset of Fig. 3d shows the EL spectra under different injection currents. The peak wavelengths are around 292 nm, which remain nearly constant with the injection current. The electrical performance of the presented DUV AlGaIn nanowire LEDs is comparable to, or better than the previously reported DUV AlGaIn quantum well LEDs in the same wavelength range^{25,26}.

Discussions

In this work, we show that N-polar catalyst-free Al(Ga)N nanowire arrays grown directly on large-area and low-cost Si substrate can

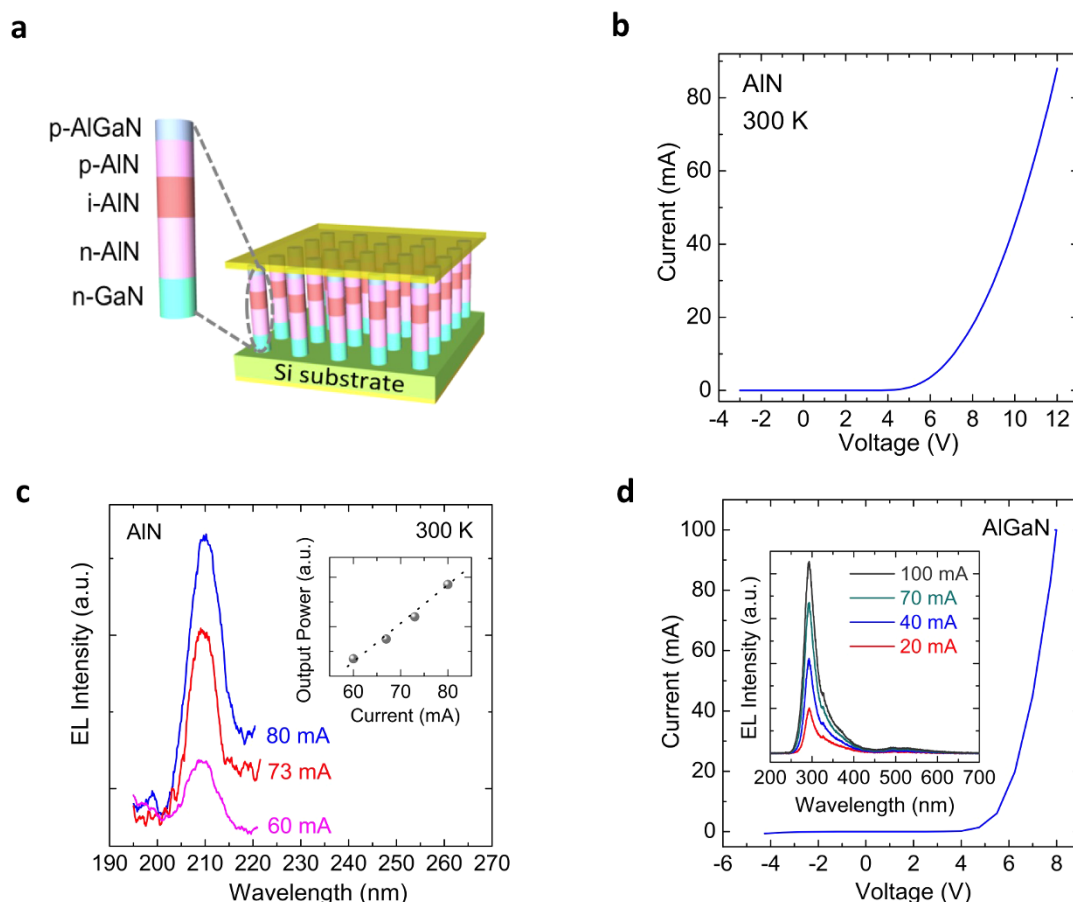


Figure 3 | Electrically injected Al(Ga)N nanowire LEDs under CW operation at room temperature. (a) The schematic illustration of AlN LED structure. (b) The I - V characteristics of AlN LEDs. (c) The EL spectra of AlN LEDs under different injection levels measured at room temperature with the inset showing the output power as a function of the injection current. (d) The I - V characteristics of AlGaIn LEDs, with the inset showing the EL spectra under different injection currents.

offer a feasible path to realize tunable DUV light sources with both ultrahigh quantum efficiency and superior electrical performance. The electrical performance of AlN nanowire LEDs, including the device resistance, may further be optimized by using graded Al compositions in the (Al)GaIn/AlN heterojunctions. In addition, it is noted that the use of nanowire structures could lead to much enhanced light extraction efficiency, compared to conventional planar LEDs, due to the large area sidewalls with their normal axis perpendicular to the c -axis. Future work includes the development of AlGaIn DUV nanowire LEDs and lasers on transparent substrates⁴⁴ for significantly improved light extraction efficiency and for high power operation.

Methods

Synthesis of AlN nanowires. Catalyst-free AlN nanowires were grown on Si substrates by radio-frequency plasma-assisted MBE under nitrogen-rich conditions. In this experiment, a GaN nanowire template was grown first, wherein a thin (0.6 nm) Ga seeding layer was deposited on Si substrates before introducing nitrogen. The Ga seeding layer forms nanoscale droplets at growth temperature, which can promote the subsequent formation and nucleation of GaN nanowires. The growth was interrupted afterwards, to reach the growth temperature of AlN nanowires³¹. The growth conditions for GaN nanowire template included a substrate temperature of 790°C, a Ga beam equivalent pressure of 6×10^{-8} Torr, a nitrogen flow rate of 1 sccm, and a RF plasma forward power of 350 W. The AlN nanowire growth temperature was 800°C, and Al fluxes were in the range of 2 – 6×10^{-8} Torr. For the AlN:Mg nanowires, Mg cell temperatures of 280°C and 340°C were employed. For the AlN LEDs, the Si cell temperature was 1250°C³⁹, and the Mg cell temperature was 280°C. With a Mg cell temperature of 280°C, the beam equivalent flux was 3×10^{-9} Torr. The Mg concentration in an equivalent AlN:Mg epilayer was $1 \times 10^{21} \text{ cm}^{-3}$ ⁴⁵. For the Al-rich AlGaIn LEDs, similar n-type and p-type doping levels were used, and the flux ratio of Al/(Al+Ga) was kept at about 72%.

Structural characterization. The SEM images were taken using a FEI F50 system. The experiments were performed with a 45-degree angle. An accelerating voltage of 5 kV was used for imaging. The TEM images were taken with a Tecnai G2 F20 S/TEM system, equipped with a Gatan 4k \times 4k CCD camera. The system has a point-to-point resolution of 0.14 nm and a line-resolution of 0.17 nm. The operation voltage is 200 kV. The cold finger is cooled with liquid nitrogen to avoid contamination.

Angle-resolved X-ray photoelectron spectroscopy. Angle-resolved X-ray photoelectron spectroscopy (ARXPS) experiments were performed in a Thermo Scientific K-Alpha system. In this experiment, an X-ray beam was impinged upon the nanowires at a 60-degree angle with respect to the nanowire c -axis, and the resulting photoelectrons were collected by an electron energy analyzer above the nanowires (near-zero take-off angle). In this configuration, the majority of the signal was derived from nanowire sidewalls. The spectra were calibrated by both Au-4f peak (84 eV) and C-1s peak (285 eV).

Emission spectra measurements. Photoluminescence (PL) measurements were performed in a homemade system. In this experiment, the nanowires were optically excited using a $\lambda = 193$ nm ArF₂ excimer laser, and the laser beam was defocused to minimize the laser damage to the sample. The spot size was about 1 mm. The emitted light from the nanowires was spectrally resolved by a high-resolution spectrometer, and was detected by a high sensitivity and low noise photomultiplier tube (PMT) in the DUV range. The electroluminescence (EL) was measured in the same setup, except the emitted light was collected by a DUV optical fiber and coupled to the same high-resolution spectrometer.

Fabrication of Al(Ga)N nanowire LEDs. Both AlN and AlGaIn LEDs were fabricated by similar processes, including a backside n-metal consisting of Ti 10 nm/Au 30 nm, and topside p-metal consisting of Ni 10 nm/Au 10 nm, which was deposited in a tilting angle.

1. Chichibu, S. F. *et al.* Origin of defect-insensitive emission probability in In-containing (Al,In,Ga)N alloy semiconductors. *Nature Mater.* **5**, 810–816 (2006).



2. Taniyasu, Y., Kasu, M. & Makimoto, T. An aluminium nitride light-emitting diode with a wavelength of 210 nanometres. *Nature* **441**, 325–328 (2006).
3. Taniyasu, Y. & Kasu, M. Polarization property of deep-ultraviolet light emission from C-plane AlN/GaN short-period superlattices. *Appl. Phys. Lett.* **99**, 251112 (2011).
4. Khan, A., Balakrishnan, K. & Katona, T. Ultraviolet light-emitting diodes based on group three nitrides. *Nature Photon.* **2**, 77–84 (2008).
5. Shur, M. S. & Gaska, R. Deep-Ultraviolet Light-Emitting Diodes. *IEEE Transcat. on Electr. Dev.* **57**, 12–25 (2010).
6. Hirayama, H. *et al.* 222–282 nm AlGaIn and InAlGaIn based deep-UV LEDs fabricated on high-quality AlN template. *Proc. of SPIE* **7216**, 721621 (2009).
7. Liao, Y. *et al.* Recent progress of efficient deep UV-LEDs by plasma-assisted molecular beam epitaxy. *Phys. Stat. Sol. (c)* **9**, 798–801 (2012).
8. Bhattacharyya, A., Moustakas, T. D., Zhou, L., Smith, D. J. & Hug, W. Deep ultraviolet emitting AlGaIn quantum wells with high internal quantum efficiency. *Appl. Phys. Lett.* **94**, 181907 (2009).
9. Kao, T.-T. *et al.* Sub-250 nm low-threshold deep-ultraviolet AlGaIn-based heterostructure laser employing HfO₂/SiO₂ dielectric mirrors. *Appl. Phys. Lett.* **103**, 211103 (2013).
10. Simon, J., Vladimir Protasenko, C. L., Xing, H. & Jena, D. Polarization-Induced Hole Doping in Wide-Band-Gap Uniaxial Semiconductor Heterostructures. *Science* **327**, 60–64 (2010).
11. Martens, M. *et al.* Performance Characteristics of UV-C AlGaIn-Based Lasers Grown on Sapphire and Bulk AlN Substrates. *IEEE Photon. Technol. Lett.* **26**, 342–345 (2014).
12. Yoshida, H., Yamashita, Y., Kuwabara, M. & Kan, H. Demonstration of an ultraviolet 336 nm AlGaIn multiple-quantum-well laser diode. *Appl. Phys. Lett.* **93**, 241106 (2008).
13. Himwas, C. *et al.* AlGaIn/AlN quantum dots for UV light emitters. *Phys. Stat. Sol. (c)* **10**, 285–288 (2013).
14. Carnevale, S. D. *et al.* Mixed Polarity in Polarization-Induced pn Junction Nanowire Light Emitting Diodes. *Nano Lett.* **13**, 3029–3035 (2013).
15. Kneissl, M. *et al.* Advances in group III-nitride-based deep UV light-emitting diode technology. *Semicond. Sci. Technol.* **26**, 014036 (2011).
16. Tsuzuki, H. *et al.* High-performance UV emitter grown on high-crystalline-quality AlGaIn underlying layer. *Phys. Stat. Sol. (a)* **206**, 1199–1204 (2009).
17. Fujikawa, S., Takano, T., Kondo, Y. & Hirayama, H. 340 nm-band high-power InAlGaIn quantum well ultraviolet light-emitting diode using p-type InAlGaIn layers. *Phys. Stat. Sol. (c)* **5**, 2280–2282 (2008).
18. Christmann, G., Butté, R. I., Feltn, E., Carlin, J.-F. o. & Grandjean, N. Room temperature polariton lasing in a GaN/AlGaIn multiple quantum well microcavity. *Appl. Phys. Lett.* **93**, 051102 (2008).
19. Takano, T., Narita, Y., Horiuchi, A. & Kawanishi, H. Room-temperature deep-ultraviolet lasing at 241.5 nm of AlGaIn multiple-quantum-well laser. *Appl. Phys. Lett.* **84**, 3567–3569 (2004).
20. Nam, K. B., Li, J., Nakarmi, M. L., Lin, J. Y. & Jiang, H. X. Unique optical properties of AlGaIn alloys and related ultraviolet emitters. *Appl. Phys. Lett.* **84**, 5264–5266 (2004).
21. Zhang, Y. *et al.* Near milliwatt power AlGaIn-based ultraviolet light emitting diodes based on lateral epitaxial overgrowth of AlN on Si(111). *Appl. Phys. Lett.* **102**, 011106 (2013).
22. Akiba, M. *et al.* Growth of flat p-GaN contact layer by pulse flow method for high light-extraction AlGaIn deep-UV LEDs with Al-based electrode. *Phys. Stat. Sol. (c)* **9**, 806–809 (2012).
23. Sekiguchi, H., Kishino, K. & Kikuchi, A. GaN/AlGaIn nanocolumn ultraviolet light-emitting diodes grown on n-(111) Si by RF-plasma-assisted molecular beam epitaxy. *Electron. Lett.* **44**, 151 (2008).
24. Hu, X. *et al.* Deep ultraviolet light-emitting diodes. *Phys. Stat. Sol. (a)* **203**, 1815–1818 (2006).
25. Allerman, A. A. *et al.* Growth and design of deep-UV (240–290nm) light emitting diodes using AlGaIn alloys. *J. Cryst. Growth* **272**, 227–241 (2004).
26. Zhang, J. P. *et al.* AlGaIn-based 280 nm light-emitting diodes with continuous-wave power exceeding 1 mW at 25 mA. *Appl. Phys. Lett.* **85**, 5532–5534 (2004).
27. Nam, K. B., Nakarmi, M. L., Li, J., Lin, J. Y. & Jiang, H. X. Mg acceptor level in AlN probed by deep ultraviolet photoluminescence. *Appl. Phys. Lett.* **83**, 878–880 (2003).
28. Taniyasu, Y., Kasu, M. & Makimoto, T. Electrical conduction properties of n-type Si-doped AlN with high electron mobility ($> 100 \text{ cm}^2 \text{ V}^{-1} \text{ s}^{-1}$). *Appl. Phys. Lett.* **85**, 4672–4674 (2004).
29. Taniyasu, Y., Kasu, M. & Makimoto, T. Increased electron mobility in n-type Si-doped AlN by reducing dislocation density. *Appl. Phys. Lett.* **89**, 182112 (2006).
30. Taniyasu, Y. & Kasu, M. Surface 210 nm light emission from an AlN p–n junction light-emitting diode enhanced by A-plane growth orientation. *Appl. Phys. Lett.* **96**, 221110 (2010).
31. Wang, Q. *et al.* Optical properties of strain-free AlN nanowires grown by molecular beam epitaxy on Si substrates. *Appl. Phys. Lett.* **104**, 223107 (2014).
32. Bertness, K. A., Sanford, N. A. & Davydov, A. V. GaN Nanowires Grown by Molecular Beam Epitaxy. *IEEE J. Select. Top. Quan. Electron.* **17**, 847–858 (2011).
33. Fernandez-Garrido, S. *et al.* Spontaneous nucleation and growth of GaN nanowires: the fundamental role of crystal polarity. *Nano Lett.* **12**, 6119–6125 (2012).
34. Hestroffer, K., Leclerc, C., Bougerol, C., Renevier, H. & Daudin, B. Polarity of GaN nanowires grown by plasma-assisted molecular beam epitaxy on Si(111). *Phys. Rev. B* **84**, 245302 (2011).
35. He, J. H. *et al.* Aligned AlN Nanorods with Multi-tipped Surfaces—Growth, Field-Emission, and Cathodoluminescence Properties. *Adv. Mater.* **18**, 650–654 (2006).
36. Xu, C., Xue, L., Yin, C. & Wang, G. Formation and photoluminescence properties of AlN nanowires. *Phys. Stat. Sol. (a)* **198**, 329–335 (2003).
37. Perea, D. E. *et al.* Direct measurement of dopant distribution in an individual vapour-liquid-solid nanowire. *Nature Nanotechnol.* **4**, 315–319 (2009).
38. Xie, P., Hu, Y., Fang, Y., Huang, J. & Lieber, C. M. Diameter-dependent dopant location in silicon and germanium nanowires. *Proc. Natl. Acad. Sci.* **106**, 15254–15258 (2009).
39. Zhao, S. *et al.* Tuning the surface charge properties of epitaxial InN nanowires. *Nano Lett.* **12**, 2877–2882 (2012).
40. Zhao, S. *et al.* p-Type InN Nanowires. *Nano Lett.* **13**, 5509–5513 (2013).
41. Nakarmi, M. L., Nepal, N., Lin, J. Y. & Jiang, H. X. Photoluminescence studies of impurity transitions in Mg-doped AlGaIn alloys. *Appl. Phys. Lett.* **94**, 091903 (2009).
42. Kawaguchi, Y. *et al.* Influence of polarity on carrier transport in semipolar (20–21) and (20–21) multiple quantum-well light emitting diodes. *Appl. Phys. Lett.* **100**, 231110 (2012).
43. Kawaguchi, Y. *et al.* Semipolar (20–21) single-quantum-well red light-emitting diodes with a low forward voltage. *Jpn. J. Appl. Phys.* **52**, 08JC08 (2013).
44. Zhao, S., Kibria, M. G., Wang, Q., Nguyen, H. P. T. & Mi, Z. Growth of large-scale vertically aligned GaN nanowires and their heterostructures with high uniformity on SiO₂ by catalyst-free molecular beam epitaxy. *Nanoscale* **5**, 5283–5287 (2013).
45. Kibria, M. G. *et al.* Tuning the surface Fermi level on p-type gallium nitride nanowires for efficient overall water splitting. *Nature Commun.* **5**, 3825 (2014).

Acknowledgments

This work was supported by the Natural Sciences and Engineering Research Council of Canada and US Army Research Office under Grant W911NF-12-1-0477. Part of the work was performed in the McGill Nanotools-Microfab facility. SEM and TEM studies were performed in the Facility for Electron Microscopy Research, McGill University.

Author contributions

S. Z. and Z. M. designed the experiments. S. Z. and Z. M. performed the Al(Ga)N nanowires growth. S. Z. performed SEM experiments. S. Z. and X. D. L. performed TEM experiments. S. Z. performed XPS experiments. S. Z., A. T. C., and Q. W. performed PL experiments. M. H. T. D., Q. W., and S. S. carried out device fabrication. S. Z., A. T. C., M. H. T. D., Q. W., and I. S. contributed to electrical injection experiments. M. D. performed polarity dependent electrical performance simulation. X. H. K. and H. G. performed theoretical calculation of Mg doping into AlN nanowires. All the authors contributed to the results analysis and discussion.

Additional information

Supplementary information accompanies this paper at <http://www.nature.com/scientificreports>

Competing financial interests: The authors declare no competing financial interests.

How to cite this article: Zhao, S. *et al.* Aluminum nitride nanowire light emitting diodes: Breaking the fundamental bottleneck of deep ultraviolet light sources. *Sci. Rep.* **5**, 8332; DOI:10.1038/srep08332 (2015).



This work is licensed under a Creative Commons Attribution-NonCommercial-NoDerivs 4.0 International License. The images or other third party material in this article are included in the article's Creative Commons license, unless indicated otherwise in the credit line; if the material is not included under the Creative Commons license, users will need to obtain permission from the license holder in order to reproduce the material. To view a copy of this license, visit <http://creativecommons.org/licenses/by-nc-nd/4.0/>